Journal of Microbiology (2022) Vol. 60, No. 11, pp. 1095–1105
DOI 10.1007/s12275-022-2284-8
eISSN 1976-3794
pISSN 1225-8873

Sulforaphane kills *Mycobacterium tuberculosis* H37Ra and *Mycobacterium smegmatis* mc^{2}155 through a reactive oxygen species dependent mechanism[§]

Yongjie Zhao[†], Shengwen Shang[†], Ya Song, Tianyue Li, Mingliang Han, Yuexuan Qin, Meili Wei, Jun Xi[*], and Bikui Tang[*]

School of Life Science, Anhui Province Key Laboratory of Immunology in Chronic Diseases, Anhui Key Laboratory of Infection and Immunity, Bengbu Medical College, Bengbu, Anhui 233030, P. R. China

(Received Jun 20, 2022 / Revised Aug 9, 2022 / Accepted Aug 22, 2022)

***Mycobacterium tuberculosis* (*M. tuberculosis*) is a highly pathogenic intracellular pathogen that causes tuberculosis (TB), the leading cause of mortality from single infections. Redox homeostasis plays a very important role in the resistance of *M. tuberculosis* to antibiotic damage and various environmental stresses. The antioxidant sulforaphane (SFN) has been reported to exhibit anticancer activity and inhibit the growth of a variety of bacteria and fungi. Nonetheless, it remains unclear whether SFN exhibits anti-mycobacterial activity. Our results showed that the SFN against *M. tuberculosis* H37Ra exhibited bactericidal activity in a time and dose-dependent manner. The anti-tubercular activity of SFN was significantly correlated with bacterial reactive oxygen species (ROS) levels. In addition, SFN promoted the bactericidal effect of macrophages on intracellular bacteria in a dose-dependent manner, mediated by increasing intracellular mitochondrial ROS levels and decreasing cytoplasmic ROS levels. Taken together, our data revealed the previously unrecognized antimicrobial functions of SFN. Future studies focusing on the mechanism of SFN in macrophages against *M. tuberculosis* are essential for developing new host-directed therapeutic approaches against TB.**

***Keywords*:** *Mycobacterium tuberculosis*, sulforaphane, redox, ROS, macrophages

Introduction

Tuberculosis (TB) is an infectious disease caused by the highly contagious pathogen *Mycobacterium tuberculosis* (*M. tuberculosis*) and is one of the leading causes of mortality from single-infection globally. In 2020, an estimated 9.9 million people developed TB, and 1.4 million died, with a quarter of the world's population latently infected with *M. tuberculosis* (WHO, 2021).

Rifampin (Rif), isoniazid (INH), pyrazinamide (PZA), and ethambutol (EMB) are first-line drugs used in TB chemotherapy for decades (Beena and Rawat, 2013; Zumla *et al.*, 2013). The current treatment for drug-sensitive TB is divided into a two-month intensive phase with first-line drugs followed by a four-month continuation phase. However, poor patient compliance and drug side effects can lead to failure of first-line drug therapy, leading to different forms of drug resistant mycobacteria, including extensively drug-resistant TB, totally drug-resistant TB, and multidrug-resistant TB, which has contributed to the increased prevalence of TB (Taati Moghadam *et al.*, 2020; Singh and Chibale, 2021). It has been established that multidrug-resistant TB patients are resistant to at least Rif and INH not sensitive to common TB drug regimens and require relatively expensive and more toxic second-line drugs for effective treatment, usually requiring a longer treatment period (minimum of up to 18 months) (Heemskerk *et al.*, 2015). These findings emphasize the need to discover new and more effective anti-TB drugs.

Disturbances in the prooxidant-antioxidant balance can cause oxidative stress leading to potential oxidative damage caused by active oxygen species attacking the composition of the biological organism (Halliwell and Gutteridge, 2007). It has been shown that both oxidative and reductive stress can induce redox cascades that alter signaling, DNA, RNA and protein synthesis and drug resistance in *M. tuberculosis*. However, *M. tuberculosis* has developed specific mechanisms to protect itself against endogenously produced oxidants such as reactive oxygen species (ROS), oxidants and reducing agents present in the host and the environment, especially in the lungs. In this regard, *M. tuberculosis* has evolved pathways similar to other bacterial species for sophisticated monitoring of redox signals such as O_2, NO, and CO and changes in the redox status inside and outside the cell (Kumar *et al.*, 2007). In addition, *M. tuberculosis* maintains intracellular redox homeostasis through mycothiol, thioredoxin, catalase-peroxidase, superoxide dismutase and other mechanisms (Kumar *et al.*, 2011). Recent studies have demonstrated that an altered redox status plays an important role in the bactericidal activity of antibiotics, as three major bactericidal antibiotics (quinolones, β-lactams, and aminoglycosides) stimulate highly harmful hydroxyl radicals produced by Gram-negative and Gram-positive bacteria via

[†]These authors contributed equally to this work.
*For correspondence. (J. Xi) E-mail: luckymq2014@foxmail.com / (B. Tang) E-mail: bikui_tang@163.com
[§]Supplemental material for this article may be found at https://doi.org/10.1007/s12275-022-2284-8.

the Fenton reaction and are the end products of oxidative damage cell death pathways (Kohanski *et al.*, 2007). Moreover, the antioxidant vitamin C (VC) can induce the reduction of trivalent iron ions to ferrous ions to produce ROS through the Fenton reaction to kill *M. tuberculosis* by inducing DNA damage. Interestingly, it has also been shown that oxidative stress response genes are upregulated in *M. tuberculosis* cells after VC treatment (Vilchèze *et al.*, 2013; Pei *et al.*, 2019).

Sulforaphane (4-methylsulfonyl butyl isothiocyanate, SFN) is a natural product with antioxidant properties derived from glucosinolates and hydrolyzed by the myrosinase enzyme in plants (Piasecka *et al.*, 2015). SFN has been reported to inhibit the growth of a range of bacterial and fungal pathogens by directly targeting the bacterial type III secretion system (Wang *et al.*, 2020). Besides, SFN pretreatment of macrophages can effectively inhibit the intracellular survival of *Staphylococcus aureus* (*S. aureus*) by reducing *S. aureus*-induced caspases-3/7-dependent apoptosis via modulation of the p38/JNK signaling pathway (Deramaudt *et al.*, 2020). Moreover, SFN has been reported to activate the Nrf2 signaling pathway to induce caspase-independent cell apoptosis to reduce the proliferation of *Mycobacterium abscessus* in macrophages (Bonay *et al.*, 2015).

Based on the above observations, we aimed to investigate the effects of SFN on *M. tuberculosis* H37Ra both *in vitro* and intracellularly. Our results showed that SFN exerted bacteriostatic effects against *Mycobacterium smegmatis* mc^{2}155 (*M. smegmatis* mc^{2}155) and *M. tuberculosis* H37Ra at low minimum inhibitory concentration (MIC) values and a bactericidal effect by upregulating the intracellular ROS levels in *M. smegmatis* mc^{2}155 and *M. tuberculosis* H37Ra in a time and dose-dependent manner *in vitro*. In addition, SFN showed much promise for host-directed therapy (HDT) by promoting the bactericidal effect of *M. smegmatis* mc^{2}155 and *M. tuberculosis* H37Ra in macrophages, enhancing mitochondrial ROS (mROS) levels and decreasing cytoplasmic ROS (cROS) levels, suggesting its role in promoting macrophage autophagy. This study showed that SFN has broad prospects as a novel treatment approach against *M. tuberculosis*, providing a new strategy for further development of anti-TB drugs.

Materials and Methods

Bacterial strains, cells culture, and reagents

The *M. smegmatis* mc^{2}155, *M. tuberculosis* H37Ra and *Escherichia coli* MG1655 (*E. coli* MG1655) strains used in this study were from ATCC. *Mycobacterium smegmatis* mc^{2}155 were grown in Middlebrook 7H9 broth medium (Difco, BD) supplemented with 0.05% (v/v) Tween 80 and 0.2% (v/v) glycerol to achieve exponential-phase (optical density at 600 nm [OD_{600}] = 0.6 to 0.8) or stationary-phase (5 days) growth at 37°C with shaking at 100 rpm or on Luria-Bertani (LB) agar supplemented with 0.5% (v/v) glycerol (LBG) for 3 days. *M. tuberculosis* H37Ra were grown in Middlebrook 7H9 broth medium with 0.05% (v/v) Tween 80 and 0.2% (v/v) glycerol supplemented with 10% oleate-albumin-dextrose-catalase (OADC) enrichment (Difco, BD) to achieve exponential-phase or on 7H10 (Difco, BD) plates supplemented with 0.5% glycerol and 10% OADC for 3 weeks. The *E. coli* MG1655 was cultured in LB broth at 37°C with shaking at 180 rpm for 8 h to achieve exponential-phase growth.

The human acute monocytic leukemia cell line THP-1 was purchased from the National Collection of Authenticated Cell Cultures, cultured in RPMI medium 1640 (Sigma-Aldrich) supplemented with 10% fetal bovine serum (Gibco) and maintained in a 37°C incubator with 5% CO_2. THP-1 cells were induced to undergo macrophage-like changes by phorbol-12-myristate-13-acetate (PMA, 20 ng/ml) for 24 h, which were then called PMA-activated THP-1 macrophages.

N-acetyl-L-cysteine (NAC), PMA, dihydroethidium (DHE), catalase (CAT), 2,7'-dichlorofluorescein-diacetate (DCFH-DA), and SFN were purchased from Sigma-Aldrich. MitoSOX was purchased from Invitrogen.

MIC determination

The MIC is the lowest drug concentration that leads to no visible growth of a bacterial strain. The MIC was determined by broth macrodilution of the drug in 96-well plates with Middlebrook 7H9 broth medium (Andrews, 2001). Briefly, exponential-phase cultures were diluted to OD_{600} 0.03 (approximately 3×10^6 cells/ml) in a medium with or without 10% OADC and exposed to different concentrations of SFN and VC in round-bottom 96-well plates. Plates were then incubated at 37°C for 1 (*E. coli* MG1655), 3 (*M. smegmatis* mc^{2}155), or 21 days (*M. tuberculosis* H37Ra).

Time-dependent killing

To evaluate the killing effect of SFN against *M. smegmatis* mc^{2}155 and *M. tuberculosis* H37Ra, cell density is controlled at approximately 1×10^7 cells/ml for the exponential-phase cultures and approximately 1×10^8 cells/ml for stationary-phase cultures. *M. smegmatis* mc^{2}155 and *M. tuberculosis* H37Ra cultures were treated with different concentrations of SFN (50, 100, 200 μg/ml for *M. smegmatis* mc^{2}155, 25, 50, 100, 200 μg/ml for *M. tuberculosis* H37Ra), 5 mM NAC, 100 U/ml CAT or 10 × MIC Rif (20 μg/ml) in 5 ml EP tubes at 37°C with headspace air volume to liquid volume ranging at 0.25 (Wayne and Hayes, 1996), air is renewed every 12 h to maintain normal aerobic growth of bacteria. The point in time when SFN and other substrates were added was defined as 0 h. At the indicated time points, the bacterial solution was shaken. Fifty microliters aliquots were removed and resuspended in 450 μl PBS and 10-fold serially diluted suspensions were plated onto LBG or 7H10 agar. After cultivation at 37°C for 3 days and 3 weeks, colonies were counted, and the CFU count was obtained.

Determination of bacterial ROS production

To investigate the role of ROS in the antibacterial activity exerted by SFN, DHE was used as mentioned in previous study (Vilchèze *et al.*, 2013). DHE was first dissolved in DMSO to prepare a 10 mM storage fluid, which was further diluted into 5 μM working solution by the medium during cell staining. *Mycobacterium smegmatis* mc^{2}155 and *M. tuberculosis* H37Ra cultures were grown to a cell density of 1×10^7 cells/ml and treated with different concentrations of SFN. One milliliter of the well-mixed specimen were collected and cen-

trifuged at 5,000 × *g* for 5 min at the indicated time points. Cells were washed with PBS and stained with DHE working solution in a 37°C water bath for 30 min in the dark. Cells were rinsed once with medium and then suspended in the medium until it was used for flow cytometry analysis on a BD Cytek DxP Athena™ (BD Biosciences). FlowJo software (Tree Star) was used to analyze the data.

Infection of THP-1 cells with *M. smegmatis* mc²155 and *M. tuberculosis* H37Ra

Infection of THP-1 cells were performed as described (Wang *et al.*, 2006), with some modification as follows. THP-1 cells (density maintained within 2.5×10^5–1×10^6 cells/ml) were cultured in complete RPMI 1640 medium and treated with 20 ng/ml PMA for 24 h, which induced macrophage-like changes in the cells. These cells are called PMA-differentiated THP-1 macrophages. The medium was replaced by a medium containing PMA for the induction of phagocytosis with fresh complete RPMI 1640 medium, and cells were infected with *M. smegmatis* mc²155 or *M. tuberculosis* H37Ra at a multiplicity of infection (MOI) of 1:5 (cells: bacteria) for 4 h. Then cells were washed three times with prewarmed RPMI 1640 to remove extracellular bacteria. RPMI 1640 containing 10% fetal bovine serum was then used for culture.

Analysis of intracellular bacterial invasion assay

Intracellular bacterial invasion was performed as described (Pei *et al.*, 2019), with some modification as follows.THP-1 cells were inoculated in 96-well plates at a density of 5×10^4 cells/well and bacteria at 37°C with 5% CO_2. Infected cells were washed three times with prewarmed PBS to remove extracellular bacteria, then infected THP-1 cells were treated with SFN (10, 50, 100, 200 μg/ml) or without SFN for different time intervals (9, 12 h for *M. smegmatis* mc²155, 24, 48 h for *M. tuberculosis* H37Ra). The cells were then lysed twice with 150 μl 0.06% SDS. Cells lysates were plated on LBG agar (*M. smegmatis* mc²155) or 7H10 agar (*M. tuberculosis* H37Ra) supplemented with 10% OADC and incubated at 37°C. After 3 days or 3 weeks of incubation, CFU were counted for *M. smegmatis* mc²155 and *M. tuberculosis* H37Ra and expressed as CFU/ml.

Determination of intracellular production of ROS

PMA-differentiated THP-1 macrophages (5×10^5 cells/ml) were cultured in 48-well plates and infected with *M. smegmatis* mc²155 or *M. tuberculosis* H37Ra (MOI of 1:5) for 4 h. Infected cells were washed three times with prewarmed PBS to remove extracellular bacteria; the infected cells were then cultured in a fresh medium with or without different concentrations of SFN for 12 h (*M. smegmatis* mc²155) or 12, 24, 48 h (*M. tuberculosis* H37Ra). The cROS was quantified by a cell-permeable fluorescent dye DCFH-DA. Quantification of mROS was performed using the MitoSOX red mitochondrial superoxide indicator. Briefly, the cells were incubated with DCFH-DA (10 μM) or MitoSOX (2.5 μM) for 30 min at 37°C in the dark, then washed in PBS (Ouyang *et al.*, 2020). All fluorescence intensities of cells were measured by flow cytometry (BD FACSAria II flow cytometer, BD Biosciences) and analyzed by FlowJo software.

Measuring LC3 protein expression level by western blotting

PMA-differentiated THP-1 macrophages were infected with or without *M. tuberculosis* H37Ra for 4 h (MOI of 1:5). After washing with PBS, the cells were cultured with or without SFN (100 μg/ml) for specified time. After quantification and denaturation, the equivalent amounts of total protein were dissolved on SDS-acrylamide gel and electrophoretically transferred to nitrocellulose membranes (Cytiva, A29932447). The membranes were blocked with 5% skim milk in TBS for 1 h and then washed trice (10 min each) with 0.5% Tween 20 in TBS (TBST) at room temperature, incubated overnight at 4°C with primary antibodies (Abclonal, A19665). The membranes washed trice with TBST, incubated with secondary antibody (Abclonal, AS014) in TBST for 1 h, and then washed trice times with TBST. Chemiluminescence signals were then developed with Immobilon Western Chemiluminescent HRP Substrate (Millipore, P90719) followed by exposure of X-ray film (Bio-Rad). Quantification of the density of bands was performed using Image Lab.

Statistical analysis

All experiments were conducted in triplicates for each treatment group, and the data of each group were expressed as mean ± standard deviation (SD). Statistical analysis was performed using GraphPad Prism 8 software. Differences between the two groups were analyzed with the student's unpaired t-test; three or more groups were compared using one-way analysis of variance (ANOVA). The significance level was expressed as $^*P \le 0.05$, $^{**}P \le 0.01$, and $^{***}P \le 0.001$ compared with the control.

Results

MIC of SFN against *M. smegmatis* mc²155 and *M. tuberculosis* H37Ra

To determine whether SFN exerts a direct antibacterial effect, we treated *M. smegmatis* mc²155, *M. tuberculosis* H37Ra and *E. coli* MG1655 with different concentrations of SFN. As shown in Table 1, the SFN MIC for *M. tuberculosis* H37Ra and *M. smegmatis* mc²155 were 5 and 10 μg/ml, respectively. Meanwhile, the MIC of the first-line antibiotics Rif and streptomycin (Str) were 0.5 and 2 μg/ml against *M. tuberculosis* H37Ra and 0.5 and 4 μg/ml against *M. smegmatis* mc²155, respectively. These findings suggest that SFN can inhibit the growth of *M. tuberculosis in vitro*, although its MIC levels are 10-fold higher than those of anti-TB drugs Rif and Str. Interestingly, we found that SFN exhibits an antibacterial effect on *E. coli* although it was less effective than on *M. smegmatis* and *M. tuberculosis*.

Table 1. MIC of SFN, Rif, Str (μg/ml)

	SFN	Rif	Str
M. tuberculosis H37Ra	5	0.5	0.5
M. smegmatis mc²155	10	2	4
E. coli MG1655	80	-*	-*

*No determination.

Time-kill kinetic curves of SFN against *M. smegmatis* mc^{2}155 and *M. tuberculosis* H37Ra

To investigate the bactericidal effect of SFN against *M. smegmatis* mc^{2}155 and *M. tuberculosis* H37Ra *in vitro*, the exponential-phase and stationary-phase *M. smegmatis* mc^{2}155 or *M. tuberculosis* H37Ra were treated with different concentrations of SFN for 6, 9, and 12 days to obtain the time-kill kinetic curve. A time and dose-response relationship were observed (Fig. 1). Interestingly, a bactericidal effect was observed on exponential-phase *M. smegmatis* mc^{2}155 *in vitro* with the lowest concentration of SFN (50 μg/ml), which decreased the CFU count of *M. smegmatis* mc^{2}155 by 2-fold logarithmic values on day 6. Further, a 100% bactericidal effect to *M. smegmatis* mc^{2}155 was observed at 100 μg/ml and

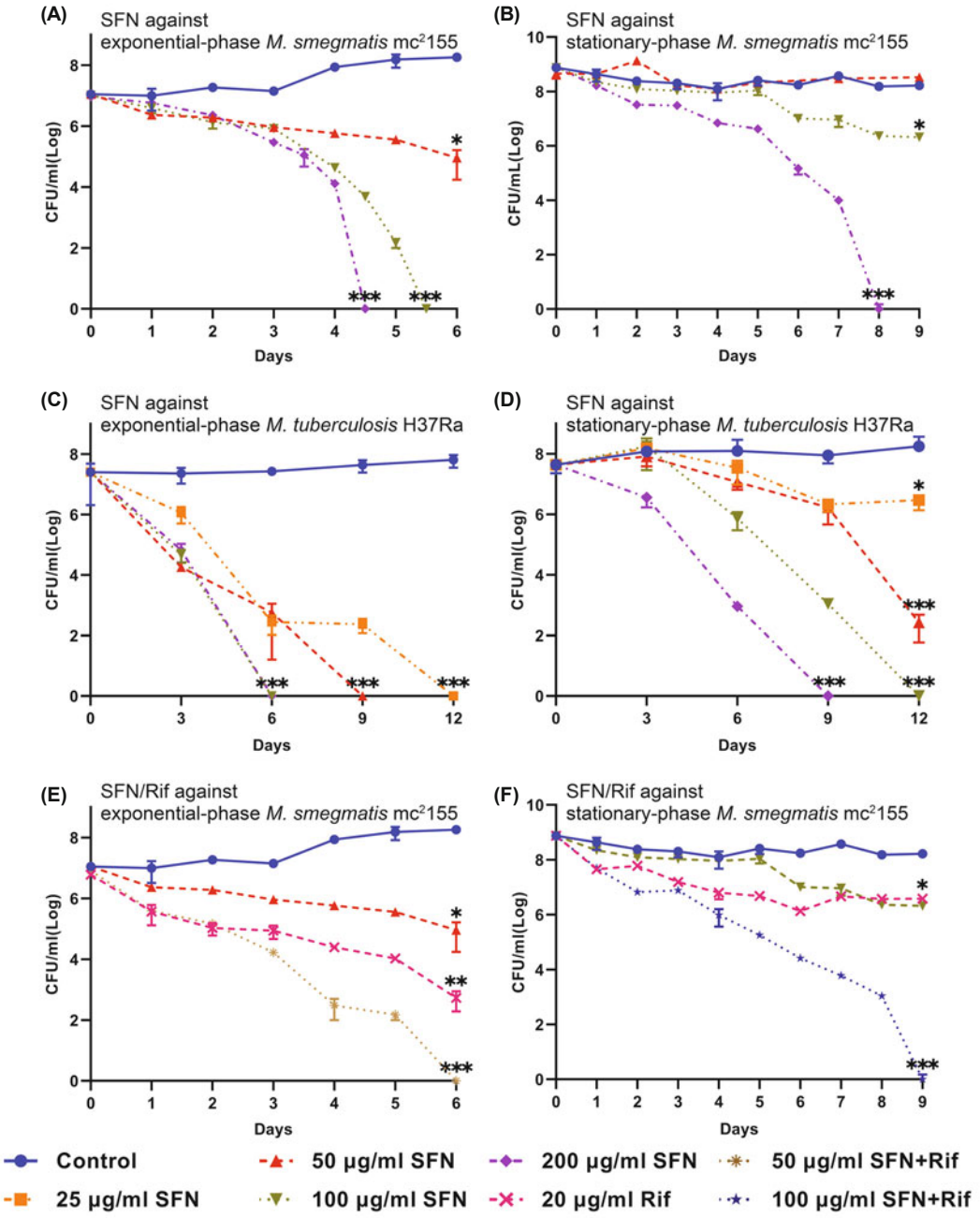

Fig. 1. SFN sterilizes *M. smegmatis* mc^{2}155 and *M. tuberculosis* H37Ra strains *in vitro*. (A) Exponential-phase *M. smegmatis* mc^{2}155 cultures or (B) stationary-phase *M. smegmatis* mc^{2}155 cultures were treated with increasing amounts of SFN (from 50 to 200 μg/ml). (C) Exponential-phase or (D) stationary-phase *M. tuberculosis* H37Ra cultures were treated with SFN (from 25 to 200 μg/ml). CFU were determined by plating tenfold serial dilutions and incubating the plates at 37°C for 3 days (for *M. smegmatis* mc^{2}155) or 21 days (for *M. tuberculosis* H37Ra). (E) Exponential-phase *M. smegmatis* mc^{2}155 cultures were treated with 20 μg/ml Rif or with a combination of Rif and SFN (50 μg/ml). (F) Stationary-phase *M. smegmatis* mc^{2}155 cultures were treated with 20 μg/ml Rif or with a combination of Rif and SFN (100 μg/ml). The data represent the means SD for three independent experiments. Compared to the control group, significance was calculated and indicated by asterisks as follows: $^*P \le 0.05$; $^{**}P \le 0.01$; $^{***}P \le 0.001$.

200 μg/ml SFN at 5.5 and 4.5 days, respectively (Fig. 1A). Interestingly, a potentiation effect with the anti-tuberculosis drug Rif was observed (Fig. 1E). Moreover, 50 μg/ml SFN exerted no significant bactericidal effect on stationary-phase *M. smegmatis* mc^{2}155; however, the CFU count was reduced by 2-fold logarithmic values on day 6 with 100 μg/ml SFN (Fig. 1B); this bactericidal effect was enhanced by Rif (Fig. 1F). 200 μg/ml SFN took longer to achieve a 100% bactericidal effect against stationary-phase *M. smegmatis* mc^{2}155 (8 days), compared with the exponential-phase mycobacteria (Fig. 1A and B). The time-kill kinetic curves of SFN against exponential-phase (Fig. 1C) or stationary-phase (Fig. 1D) *M. tuberculosis* H37Ra strain showed consistent results; 25, 50, 100, and 200 μg/ml SFN could kill all mycobacteria within 12 days.

In a nutshell, SFN at different experimental concentrations exhibited a very strong bactericidal effect against *M. smegmatis* mc^{2}155 and *M. tuberculosis* H37Ra at all growth stages. Our findings indicate that SFN has potential antibacterial activity *in vitro,* enhanced by co-administration with the known mycobactericidal drug Rif.

ROS inhibitors modulate SFN killing *in vitro*

To determine the underlying mechanisms of SFN in killing *M. smegmatis* mc^{2}155 *and M. tuberculosis* H37Ra and preliminarily analyze whether ROS play a significant role in this phenomenon, membrane-impermeant ROS scavengers NAC and CAT were used. It was found that 5 mM NAC did not significantly affect the growth of *M. smegmatis* mc^{2}155, but the killing effect of SFN on *M. smegmatis* mc^{2}155 could be completely antagonized to the level of the NAC when the two were used together (Fig. 2A). Meanwhile, another ROS inhibitor, CAT, exhibited no influence on the bactericidal effect of SFN (Fig. 2B). Those results indicated that ROS was the effector species mediating SFN-induced *M. smegmatis* mc^{2}155 death. It is widely acknowledged that CAT only catalyzes the decomposition of hydrogen peroxide (Supplementary data Fig. S1). The different observations associated with CAT and NAC can be explained by their mechanism of action. Given that CAT only acts on peroxides and NAC acts on superoxide radicals, it is thought that the killing effect of SFN on *M. smegmatis* mc^{2}155 was mainly related to superoxide radicals rather than peroxides.

Besides, the bactericidal effect of SFN (25, 50, and 100 μg/ml) against the exponential-phase *M. tuberculosis* H37Ra strain was moderately antagonized by NAC. A 3-fold logarithmic increase in the number of *M. tuberculosis* H37Ra CFU was observed on days 6, 9, and 12; however, NAC exerted no obvious effect with 200 μg/ml SFN *in vitro* (Fig. 2C). Conversely, NAC substantially antagonized the bactericidal effect of SFN on stationary-phase *M. tuberculosis* H37Ra (Fig. 2D), suggesting that ROS may play a major role in the killing of *M. tuberculosis*, especially for mycobacteria that grow at a slower rate.

SFN facilitates *M. smegmatis* mc^{2}155 and *M. tuberculosis* H37Ra generation of ROS

It has been suggested that a common mechanism of bacter-

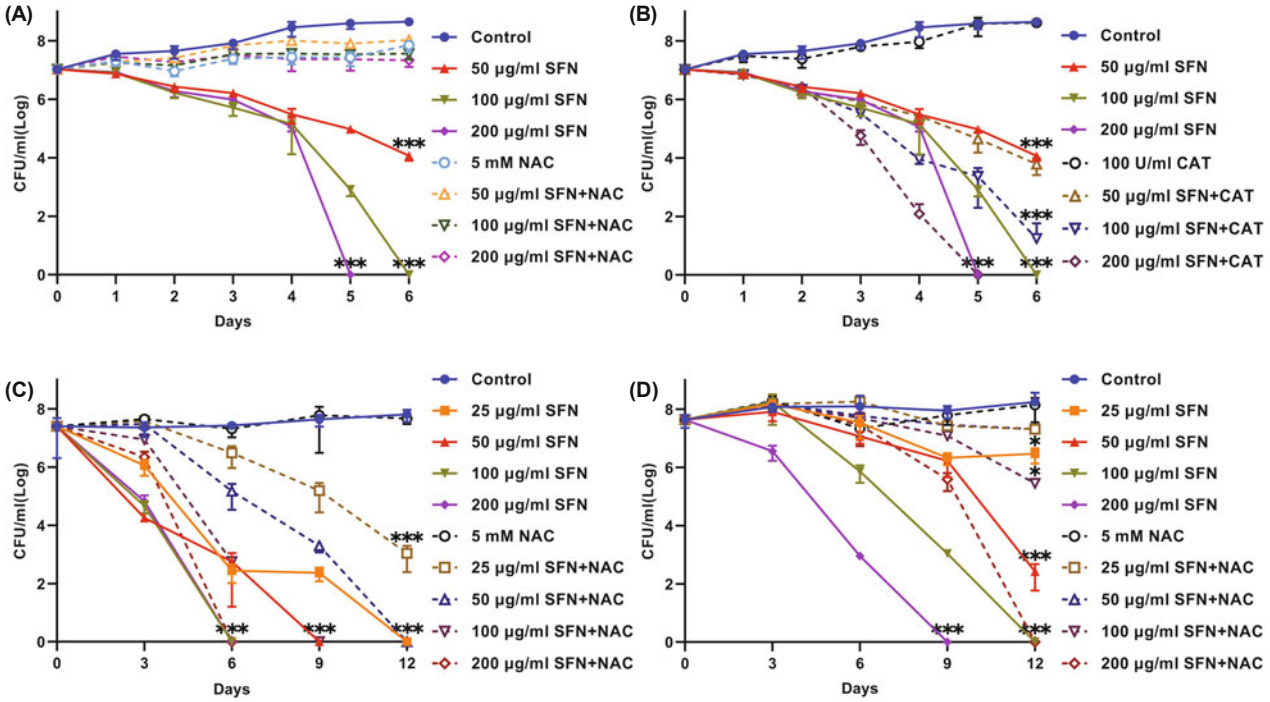

Fig. 2. SFN bacteriostatic activity was modulated by ROS inhibitors. Exponential-phase *M. smegmatis* mc^{2}155 cultures were treated with different concentrations of SFN (from 50 to 200 μg/ml) with or without 5 mM NAC (A) or 100 U/ml CAT (B). (C) Exponential-phase or (D) Stationary-phase *M. tuberculosis* H37Ra cultures were treated with SFN (from 25 to 200 μg/ml) with or without 5 mM NAC. Then, CFU were then determined. The data represent the means SD for three independent experiments. Compared to the control group, significance was calculated and indicated by asterisks as follows: *$P \leq 0.05$; ***$P \leq 0.001$.

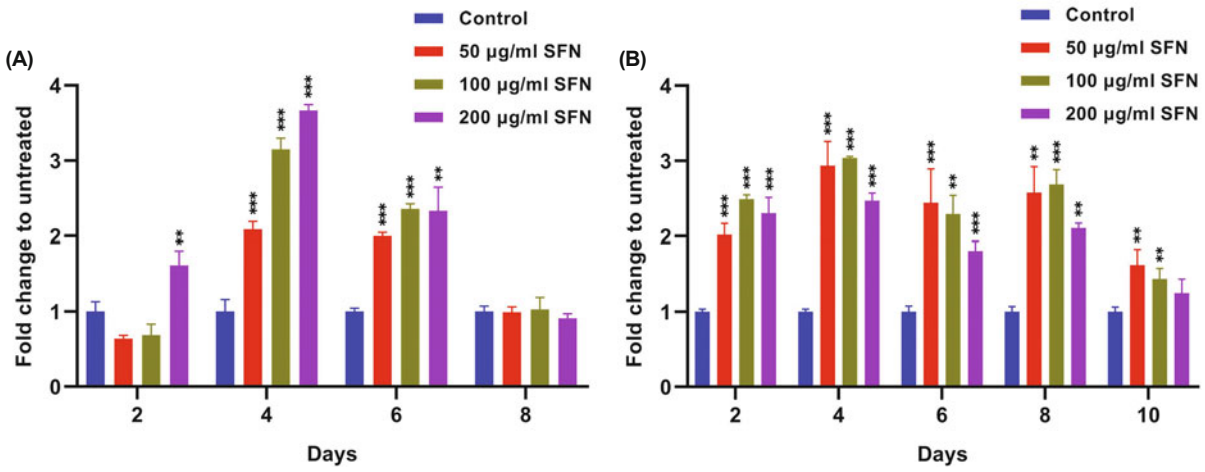

Fig. 3. SFN increases ROS levels of *M. smegmatis* mc²155 and *M. tuberculosis* H37Ra. Exponential-phase *M. smegmatis* mc²155 (A) or *M. tuberculosis* H37Ra (B) cultures were treated with different concentrations of SFN (from 50 to 200 μg/ml) and stained with dihydroethidium for ROS detection at indicated times points. The total ROS concentrations were then measured by flow cytometry as described in the Methods section. The data represent the means SD for three independent experiments. Compared to the control group, significance was calculated and indicated by asterisks as follows: $^{**}P \leq 0.01$; $^{***}P \leq 0.001$.

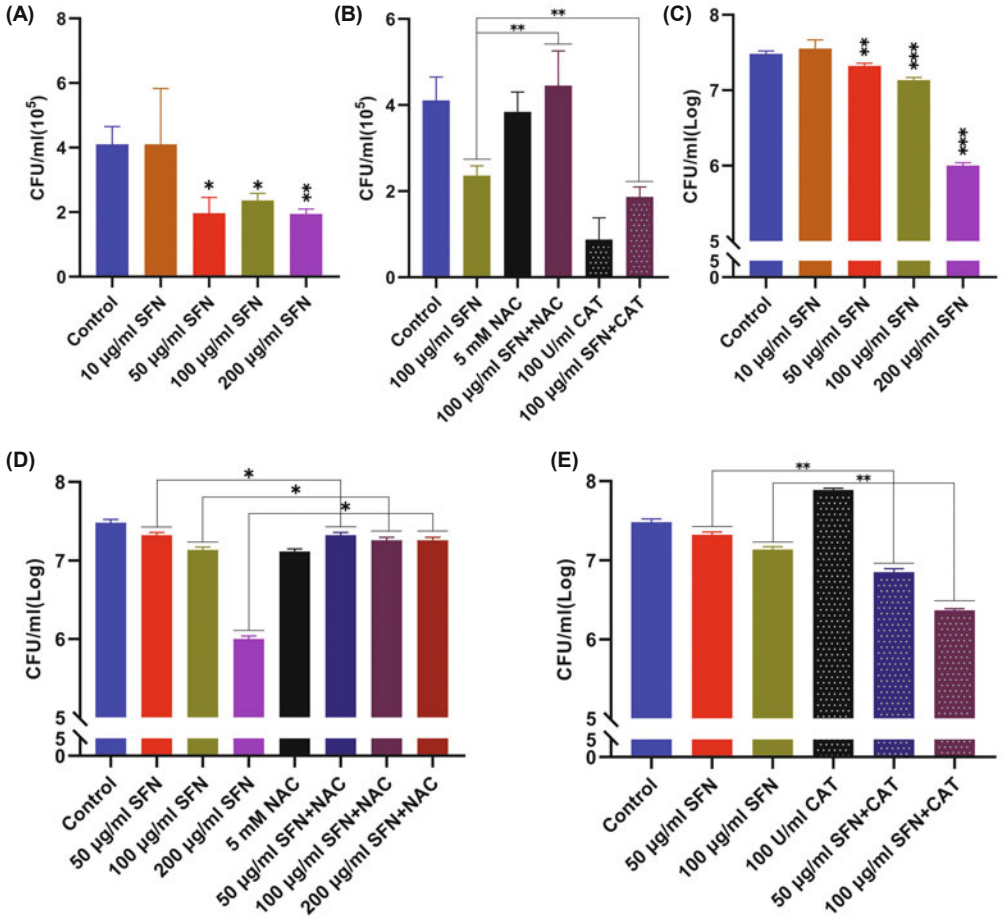

Fig. 4. SFN kills intracellular *M. smegmatis* mc²155 and *M. tuberculosis* H37Ra and is regulated by ROS inhibitors. (A) *M. tuberculosis* H37Ra infected macrophages were treated with different concentrations of SFN (from 10 to 200 μg/ml) for 48 h. (B) *M. smegmatis* mc²155 infected macrophages were treated with different concentrations of SFN (from 10 to 200 μg/ml) for 12 h. (C) *M. tuberculosis* H37Ra infected macrophages treated with 100 μg/ml SFN for 48 h with or without 5 mM NAC or 100 U/ml CAT. *Mycobacterium smegmatis* mc²155 infected macrophages treated with 50 to 200 μg/ml SFN for 12 h with or without 5 mM NAC (D) or 100 U/ml CAT (E). Macrophages lysed twice with 0.06% SDS; cells lysates were collected then CFU counts were determined. The data represent the means SD for three independent experiments. Compared to the control group, significance was calculated and indicated by asterisks as follows: $^{*}P \leq 0.05$; $^{**}P \leq 0.01$; $^{***}P \leq 0.001$.

icidal drugs involves the production of ROS via the Fenton reaction, leading to DNA damage in bacteria (Kohanski *et al.*, 2007), but another group of researchers claims that ROS do not play a role in killing bacterial pathogens with antibiotics (Keren *et al.*, 2013; Liu and Imlay, 2013). In the aforementioned *in vitro* time-kill assay, when the ROS inhibitor NAC was used to antagonize the bactericidal effect of SFN, a close correlation with ROS was demonstrated. To further investigate the role of ROS in the bactericidal effect of SFN against *M. smegmatis* mc^{2}155 and *M. tuberculosis* H37Ra, the ROS levels in *M. smegmatis* mc^{2}155 and *M. tuberculosis* H37Ra treated with different concentrations of SFN were detected by flow cytometry. A time and dose-dependent trend in ROS levels were observed (Fig. 3A). Besides, a significant increase in intracellular ROS levels of *M. smegmatis* mc^{2}155 was observed after two days at 50, 100, and 200 μg/ml of SFN, peaking on day 4 and then gradually decreasing to levels similar to the control group. The trend of intracellular ROS level of *M. smegmatis* mc^{2}155 was associated with *in vitro* killing assay (Fig. 1A), further demonstrating that SFN's bactericidal effect involved promoting ROS synthesis in *M. smegmatis* mc^{2}155. Consistently, the same concentration of SFN induced a two to three-fold increase in intracellular ROS levels in *M. tuberculosis* H37Ra during the rapid killing phase, which gradually decreased later (Fig. 3B).

SFN promotes intracellular killing by macrophages

THP-1 macrophages were pre-infected with *M. smegmatis* mc^{2}155 or *M. tuberculosis* H37Ra for 4 h and treated with SFN, CAT, or NAC for a predefined time. Then, the intracellular *M. smegmatis* mc^{2}155 and *M. tuberculosis* H37Ra was released, and the total number of colonies was counted. As shown in Fig. 4, lower concentrations of SFN (10 μg/ml) had no significant effect on the intracellular killing of THP-1 macrophages after SFN treatment for 48 h. Conversely, SFN exhibited significant intracellular *M. tuberculosis* H37Ra bactericidal efficacy at higher concentrations (50, 100, and 200 μg/ml) (Fig. 4A). A similar trend was observed during the time-kill kinetics assay of SFN on *M. smegmatis* mc^{2}155 for 12 h (Fig. 4B). Consistent with the time-kill assay *in vitro*, the enhanced bactericidal effect on intracellular *M. smegmatis* mc^{2}155 after treatment with SFN for 12 h was completely antagonized by NAC (Fig. 4D). Interestingly, this effect was enhanced by CAT when the SFN concentration did not exceed 100 μg/ml but not at 200 μg/ml (Fig. 4E). Nevertheless, the antagonistic effect of CAT against SFN was not significant *in vitro* (Fig. 2B). A similar pattern was observed after treatment with SFN for 9 h (Supplementary data Fig. S2A and B). Importantly, NAC and CAT exerted similar effects on the killing of *M. tuberculosis* H37Ra following treatment with SFN for 24 h (Supplementary data Fig. S2C) or 48 h (Fig. 4C). The difference between *in vitro* and intracellular CAT potency suggests that the intracellular bactericidal mechanism for THP-1 macrophages may differ from the *in vitro* mechanism. The enhanced intracellular bactericidal effect exerted by SFN may be related to the decline of intracellular hydrogen peroxide levels.

Effect of SFN on intracellular ROS levels

The role of ROS during the killing of *M. smegmatis* mc^{2}155 by SFN was confirmed by the *in vitro* time-kill assay. Moreover, the intracellular time-kill assay suggested the role of

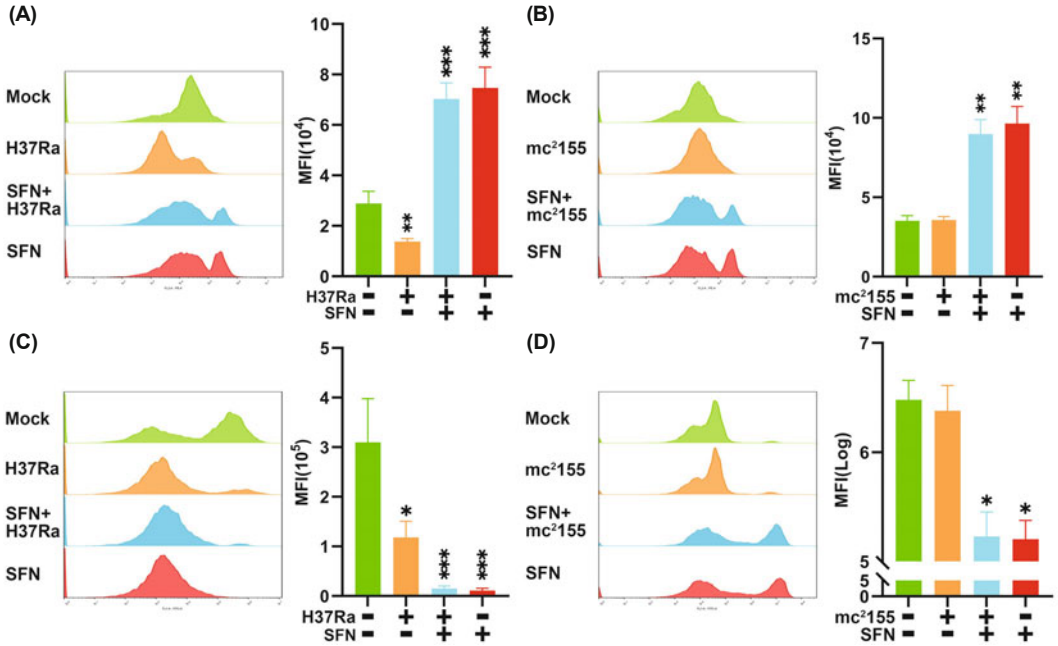

Fig. 5. SFN increased mROS and reduced cROS in macrophages. *Mycobacterium tuberculosis* H37Ra (A) or *M. smegmatis* mc^{2}155 (B) infected macrophages were treated with 100 μg/ml SFN for 12 h. mROS was quantified using MitoSOX red mitochondrial superoxide indicator. *Mycobacterium tuberculosis* H37Ra (C) or *M. smegmatis* mc^{2}155 (D) infected macrophages were treated with 100 μg/ml SFN for 12 h. cROS was quantified by DCFH-DA. MFI: Mean Fluorescence Intensity. The data represent the means SD for three independent experiments. Compared to the control group, significance was calculated and indicated by asterisks as follows: *$P \leq 0.05$; **$P \leq 0.01$; ***$P \leq 0.001$.

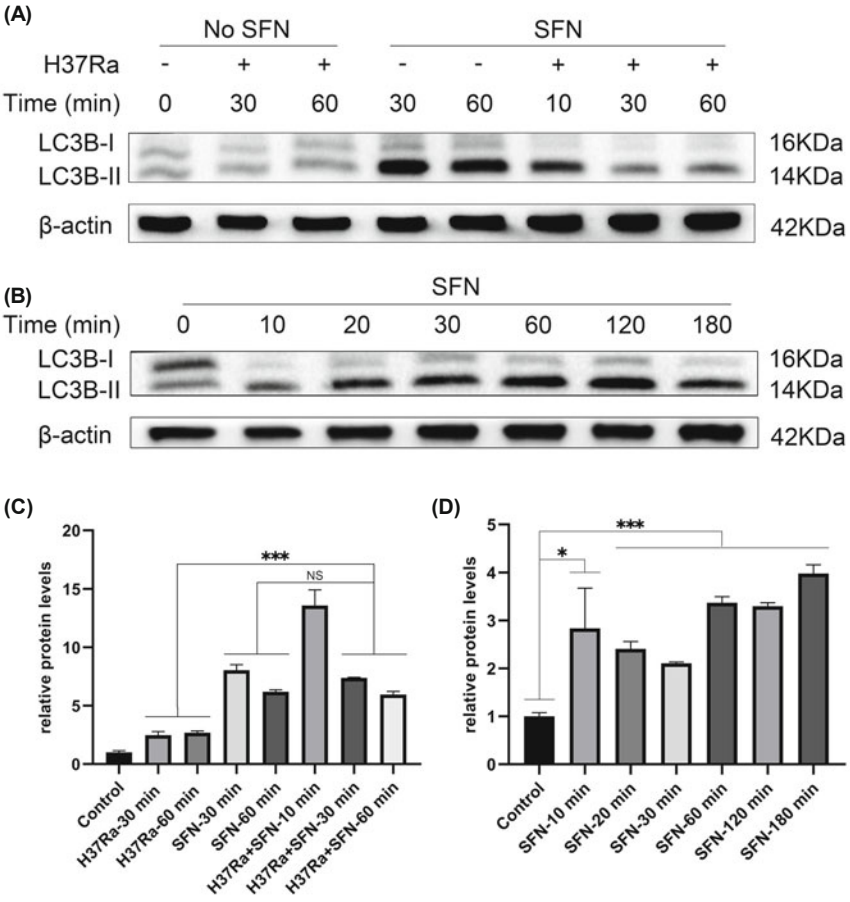

Fig. 6. SFN promotes autophagy of THP-1 macrophages. (A) Macrophages infected with or without *M. tuberculosis* H37Ra were treated with SFN (100 μg/ml) for indicated time points to detect the expression of autophagy marker proteins LC3B-I and LC3B-II. (B) Macrophages without *M. tuberculosis* H37Ra infection were treated with SFN for 0, 10, 20, 30, 60, 120, 180 min to detect the expression of autophagy marker proteins LC3B-I and LC3B-II. (C) The LC3B-I and LC3B-II levels of (A) were quantified by bands density. (D) The LC3B-I and LC3B-II levels of (B) were quantified by bands density. Significance was calculated and indicated by asterisks as follows: $^{*}P \leq 0.05$; $^{***}P \leq 0.001$.

ROS in enhancing intracellular bacterial killing by SFN. To further clarify the mechanisms underlying the regulatory role of SFN in the killing of intracellular bacteria by macrophages, we investigated the effects of SFN on *M. smegmatis* mc^{2}155 and *M. tuberculosis* H37Ra induced THP-1 macrophage ROS production, a key mechanism associated with macrophage killing of invading intracellular pathogens. We found that mitochondrial ROS (mROS) levels were significantly increased in *M. tuberculosis* H37Ra-infected macrophages (approximately four times higher) (Fig. 5A) or *M. smegmatis* mc^{2}155-infected macrophages (approximately two times higher) (Fig. 5B) after treatment with 100 μg/ml of SFN for 12 h. A similar trend was observed for mROS levels of *M. tuberculosis* H37Ra-infected macrophages after SFN treatment for 24 and 48 h (Supplementary data Fig. S3A and B). However, cROS was significantly decreased in *M. smegmatis* mc^{2}155 and *M. tuberculosis* H37Ra-infected macrophages upon treatment with 100 μg/ml SFN at the same time points (Fig. 5C and D). Subsequently, the cROS-lowering effect of SFN gradually diminished (Supplementary data Fig. S3C and D). The changes in intracellular ROS levels are highly suggestive of the role of autophagy during the intracellular killing of mycobacteria.

SFN promotes autophagy in THP-1 macrophages independent of *M. tuberculosis* H37Ra

Superoxide is the main ROS regulating autophagy (Dong *et al.*, 2019). To investigate whether the effect of SFN on cytoplasmic and mitochondrial ROS levels in THP-1 macrophages is related to autophagy occurrence, we detected expression of the autophagy marker protein LC3B. As the result shows (Fig. 6), *M. tuberculosis* H37Ra induced moderate autophagy in macrophages, whereas treatment with SFN significant promoted the conversion of autophagy marker protein LC3B-I to LC3B-II. Interestingly, SFN-induced autophagy was not significantly correlated with *M. tuberculosis* H37Ra (Fig. 6A and C). It was further found that the effect of SFN on promoting autophagy in macrophages started rapidly from 10 min after treatment and gradually increased within 180 min (Fig. 6B and D), suggesting that enhanced autophagy contributes to SFN-mediated sterilization of intracellular *M. tuberculosis* H37Ra.

Discussion

Numerous studies have confirmed that SFN possesses antitumor properties against pancreatic, lung, breast, kidney, prostate and colon cancers, exerting anti-inflammatory activity, cell cycle arrest and apoptosis-inducing effects (Jiang *et al.*, 2018; Vanduchova *et al.*, 2019). In addition, SFN exerts antibacterial activity, especially against Gram-positive bacteria. Besides, SFN is bactericidal against transiently exposed *Helicobacter pylori* (*H. pylori*) and eliminates intracellular

H. pylori from human epithelial cell lines (Fahey *et al.*, 2002; Cierpial *et al.*, 2020); however, its specific mechanism of action remains unknown. In this study, we found that SFN significantly inhibited the growth of *M. tuberculosis* H37Ra and exhibited a bactericidal effect *in vitro*. In this regard, previous studies have shown that SFN effectively inhibited the growth of various Gram-positive and Gram-negative bacteria with MIC ranging from 1–4 μg/ml *in vitro* (Johansson *et al.*, 2008). Consistently, we found that SFN exhibited antibacterial activity against *M. tuberculosis* H37Ra at a MIC of 5 μg/ml. However, the inhibitory activity of SFN against *M. tuberculosis* H37Ra has been largely understudied, warranting further studies. Our study characterized the bactericidal activity of SFN against *M. smegmatis* mc^{2}155 and *M. tuberculosis* H37Ra and found that high doses of SFN exhibited strong bactericidal activity against *M. smegmatis* mc^{2}155 and *M. tuberculosis* H37Ra *in vitro*. SFN showed significant bactericidal activity against exponential and stationary-phase *M. smegmatis* mc^{2}155 and *M. tuberculosis* H37Ra in a time and dose-dependent manner. Nonetheless, bactericidal activity against stationary-phase *M. smegmatis* mc^{2}155 and *M. tuberculosis* H37Ra was slightly weaker than exponential-phase *M. smegmatis* mc^{2}155 and *M. tuberculosis* H37Ra requiring longer treatment times and increased drug concentration. This phenomenon can be explained by the reduced efficacy of antibiotics against bacteria that do not replicate or replicate slowly during the stationary phase, regardless of the genotypic susceptibility status. It has also been established that INH and Str are more effective against actively replicating *M. tuberculosis* than non-dividing ones (Xie *et al.*, 2005; Warner and Mizrahi, 2006; De Steenwinkel *et al.*, 2010).

When the ROS scavenger NAC was added in the present study, SFN no longer exhibited antibacterial effects (Fig. 2A). Studies have shown a greater than 2-fold logarithmic reduction in CFU counts in *M. tuberculosis* H37Rv cultures treated with NAC 10 mM at 5 days and complete elimination from the culture after 7 days. Normal growth of *M. tuberculosis* H37Rv was observed at 1 mM NAC (Amaral *et al.*, 2016). In our experiment, slight inhibition of the growth of *M. smegmatis* mc^{2}155 (less than 1 logarithmic value) was observed at 5 mM NAC, while it had no significant effects on the growth of *M. tuberculosis* H37Ra. In the presence of NAC, the antibacterial effect of SFN on *M. smegmatis* mc^{2}155 under experimental concentrations was antagonized (Fig. 2A). Meanwhile, a 3-fold logarithmic increase in *M. tuberculosis* H37Ra CFU count was observed at low concentrations of SFN (no more than 100 μg/ml), while NAC exhibit limited ability to decrease ROS levels in response to high concentrations of SFN (200 μg/ml) (Fig. 2C), suggesting that ROS is the main mechanism by which SFN kills *M. smegmatis* mc^{2}155, but not for *M. tuberculosis* H37Ra. Unlike NAC, CAT did not regulate the antibacterial effect of SFN, which could be attributed to the fact that CAT can act on peroxide and hydrogen peroxide. In contrast, NAC acts only on superoxide radicals, not peroxide (Aldini *et al.*, 2018). We further demonstrated that SFN exerts its bactericidal effect by enhancing the production of superoxide radicals. In previous studies, *M. smegmatis* mc^{2}155 and *M. tuberculosis* H37Ra ROS levels were assessed by dihydroethidium (DHE) to confirm the role of ROS in SFN bactericidal activity. Intracellular ROS levels of *M. smegmatis* mc^{2}155 and *M. tuberculosis* H37Ra were significantly elevated during the rapid killing and then gradually decreased to levels similar to the control (Fig. 3). Importantly, high ROS levels can induce DNA damage and lead to cell death (Kohanski *et al.*, 2007; Lee and Lee, 2014; Tian *et al.*, 2018; Hong *et al.*, 2020).

Upon infection, mycobacteria are recognized by the host's intrinsic immune cells, triggering a series of intracellular processes that promote mycobacterial killing (Kilinç *et al.*, 2021). However, the emergence of drug-resistant TB has facilitated the development of a new model of TB drug development involving therapeutic modulation of host cell function to improve the eradication of intracellular invading pathogens, termed HDT. Given that HDT has a completely different mechanism of action than antibiotics that directly kill *M. tuberculosis*, HDT has emerged as an attractive strategy for shortening the duration of treatment and treating patients with drug-resistant TB (Kaufmann *et al.*, 2018). As our knowledge of the host response during infection has improved over the years, several pathways targeting HDT in TB have been described, such as the autophagic, cholesterol, eicosanoid, and sarcoid pathways. The mechanism of each target may vary depending on the HDT compound (Palucci and Delogu, 2018). In this regard, flunarizine has been shown to enhance the bactericidal ability of macrophages against *M. tuberculosis* via HDT (Mo *et al.*, 2021).

The role of SFN in reducing the intracellular bacterial burden of macrophages via apoptotic and autophagic pathways has been well characterized (Bonay *et al.*, 2015; Deramaudt *et al.*, 2020). Nonetheless, there is a gap in research on the anti-tubercular effects of SFN via the HDT approach. In this study, we found that 50 μg/ml SFN could promote macrophage killing of intracellular *M. smegmatis* mc^{2}155 and *M. tuberculosis* H37Ra and could be antagonized to varying degrees by NAC, consistent with the *in vitro* time-kill assay results. Interestingly, in contrast with NAC, the enhancing effect of SFN exhibited a synergistic effect with CAT (Fig. 4). In addition to its antioxidant function, NAC also possesses potent anti-mycobacterial activity. Consistently, in our study, bacterial growth was significantly inhibited after treatment with NAC. Unlike the synergistic activity of NAC with the three major classes of antibiotics, SFN may exert its bactericidal effect on intracellular *M. smegmatis* mc^{2}155 and *M. tuberculosis* H37Ra through a different pathway, namely the redox pathway.

After entering macrophages through mannose receptors, *M. tuberculosis* can regulate the release of peroxisome catalase to convert toxic H_2O_2 into water and molecular oxygen, thus inhibiting an increase in endogenous ROS (Ganguli *et al.*, 2019). Thus, exogenous CAT can promote the intracellular survival of *M. smegmatis* mc^{2}155-infected macrophages (Fig. 4E). However, the reverse is true for *M. tuberculosis* H37Ra-infected macrophages (Fig. 4C). We found that CAT, unlike NAC, could promote the intracellular bactericidal effect of SFN, possibly related to the reduction in intracellular H_2O_2 levels. The intracellular ROS assay validated our hypothesis that SFN significantly promoted elevated mROS levels in *M. smegmatis* mc^{2}155 and *M. tuberculosis* H37Ra infected macrophages and decreased cROS levels (Fig. 5). Of note, the data show that SFN alters ROS in macrophages regardless of

the presence of mycobacteria, this suggests that SFN itself has a strong ability to alter host ROS. As in contrast to the results of Li *et al.* (2021) who found that low molar concentrations of SFN (15 μM) induced only a moderate increase in ROS, a more dramatic increase in ROS was observed when mitochondria were damaged. Suggesting that SFN concentration-related alterations in host intracellular ROS levels. In the present study, MitoSOX was used to detect mROS levels, especially superoxide radicals, and DCFH-DA to measure cROS levels. Moreover, it has been established that NAC acts on mitochondrial superoxide radicals and CAT on cytoplasmic H_2O_2. It is generally accepted that one of the main sources of ROS is the substrate end of the respiratory chain in the mitochondrial inner membrane. Mitochondrial complexes can leak electrons, causing the partial reduction of oxygen to $O_2^{\bullet-}$, which then disambiguates very rapidly into H_2O_2 spontaneously or through superoxide dismutase (SOD)-mediated catalysis (Filomeni *et al.*, 2015). Existing studies have shown that increased mROS levels reduce H_2O_2 levels and increase autophagy (Chen *et al.*, 2009). Besides, SFN can activate Nrf2, decrease cROS and increase autophagy in BEAS-2BR cells (Wang *et al.*, 2018). These results suggest that SFN's intracellular killing effect is related to enhanced macrophage autophagy, warranting further *in vivo* autophagy investigations. The investigators found that up to 500 μg/ml of SFN-containing solution was not toxic to RAW 264.7 cells (Choi *et al.*, 2014), and unlike some investigators who studied the effect of low concentrations of SFN on cell (Hong *et al.*, 2020; Li *et al.*, 2021). Our experiments confirmed that low concentration of SFN promotes autophagy in macrophages within a short period of time in the presence or absence of *M. tuberculosis* H37Ra infection (Fig. 6).

Conclusion

In summary, we demonstrated that SFN kills *M. tuberculosis* H37Ra by promoting ROS production and significantly inhibits the growth of intracellular *M. tuberculosis* H37Ra by modulating macrophage ROS levels *in vitro*. These findings suggest that SFN may be an effective bactericidal approach against *M. tuberculosis* and a host-directed drug candidate for treatment. Subsequent analysis of downstream events caused by elevated ROS, such as testing whether ROS directly causes cell death by damaging DNA and the link between ROS-induced autophagy and killing intracellular bacteria, is needed to further support our current conclusion.

Acknowledgements

This work was supported by Anhui Provincial Natural Science Foundation (2108085J17, 2108085QH351), Program of BBMC (by51201310, BYLK201820), Natural Science Research Project of Anhui Educational Committee (KJ2020A0556), Excellent Talents Supporting Plan in Universities of Anhui Province (gxyq2021189), Key Research and Development Program of Anhui (201904A07020022), and Training Programs of Innovation and Entrepreneurship (Byycx20014, Byycx21047, 202010367032, 202110367021).

Conflict of Interest

The authors declare no conflict of interest.

References

Aldini, G., Altomare, A., Baron, G., Vistoli, G., Carini, M., Borsani, L., and Sergio, F. 2018. N-Acetylcysteine as an antioxidant and disulphide breaking agent: the reasons why. *Free Radic. Res.* **52**, 751–762.

Amaral, E.P., Conceição, E.L., Costa, D.L., Rocha, M.S., Marinho, J.M., Cordeiro-Santos, M., D'Império-Lima, M.R., Barbosa, T., Sher, A., and Andrade, B.B. 2016. N-Acetyl-cysteine exhibits potent anti-mycobacterial activity in addition to its known anti-oxidative functions. *BMC Microbiol.* **16**, 251.

Andrews, J.M. 2001. Determination of minimum inhibitory concentrations. *J. Antimicrob. Chemother.* **48**, 5–16.

Beena and Rawat, D.S. 2013. Antituberculosis drug research: a critical overview. *Med. Res. Rev.* **33**, 693–764.

Bonay, M., Roux, A.L., Floquet, J., Retory, Y., Herrmann, J.L., Lofaso, F., and Deramaudt, T.B. 2015. Caspase-independent apoptosis in infected macrophages triggered by sulforaphane via Nrf2/p38 signaling pathways. *Cell Death Discov.* **1**, 15022.

Chen, Y., Azad, M.B., and Gibson, S.B. 2009. Superoxide is the major reactive oxygen species regulating autophagy. *Cell Death Differ.* **16**, 1040–1052.

Choi, W.J., Kim, S.K., Park, H.K., Sohn, U.D., and Kim, W. 2014. Anti-inflammatory and anti-superbacterial properties of sulforaphane from shepherd's purse. *Korean J. Physiol. Pharmacol.* **18**, 33–39.

Cierpiał, T., Kiełbasiński, P., Kwiatkowska, M., Łyzwa, P., Lubelska, K., Kuran, D., Dąbrowska, A., Kruszewska, H., Mielczarek, L., Chilmonczyk, Z., *et al.* 2020. Fluoroaryl analogs of sulforaphane - A group of compounds of anticancer and antimicrobial activity. *Bioorg. Chem.* **94**, 103454.

De Steenwinkel, J.E.M., de Knegt, G.J., ten Kate, M.T., van Belkum, A., Verbrugh, H.A., Kremer, K., van Soolingen, D., and Bakker-Woudenberg, I.A.J.M. 2010. Time-kill kinetics of anti-tuberculosis drugs, and emergence of resistance, in relation to metabolic activity of *Mycobacterium tuberculosis*. *J. Antimicrob. Chemother.* **65**, 2582–2589.

Deramaudt, T.B., Ali, M., Vinit, S., and Bonay, M. 2020. Sulforaphane reduces intracellular survival of *Staphylococcus aureus* in macrophages through inhibition of JNK and p38 MAPKinduced inflammation. *Int. J. Mol. Med.* **45**, 1927–1941.

Dong, C., Zhou, J., Wang, P., Li, T., Zhao, Y., Ren, X., Lu, J., Wang, J., Holmgren, A., and Zou, L. 2019. Topical therapeutic efficacy of ebselen against multidrug-resistant *Staphylococcus aureus* LT-1 targeting thioredoxin reductase. *Front. Microbiol.* **10**, 3016.

Fahey, J.W., Haristoy, X., Dolan, P.M., Kensler, T.W., Scholtus, I., Stephenson, K.K., Talalay, P., and Lozniewski, A. 2002. Sulforaphane inhibits extracellular, intracellular, and antibiotic-resistant strains of *Helicobacter pylori* and prevents benzo[a]pyrene-induced stomach tumors. *Proc. Natl. Acad. Sci. USA* **99**, 7610–7615.

Filomeni, G., De Zio, D., and Cecconi, F. 2015. Oxidative stress and autophagy: the clash between damage and metabolic needs. *Cell Death Differ.* **22**, 377–388.

Ganguli, G., Mukherjee, U., and Sonawane, A. 2019. Peroxisomes and oxidative stress: their implications in the modulation of cellular immunity during mycobacterial infection. *Front. Microbiol.* **10**, 1121.

Halliwell, B. and Gutteridge, J.M. 2007. Free Radicals in Biology and Medicine. 4th edn. Oxford University Press, New York, USA.

Heemskerk, D., Caws, M., Marais, B., and Farrar, J. 2015. Tuberculosis in Adults and Children. Springer, London, United Kingdom.

Hong, Y., Li, Q., Gao, Q., Xie, J., Huang, H., Drlica, K., and Zhao, X. 2020. Reactive oxygen species play a dominant role in all pathways of rapid quinolone-mediated killing. *J. Antimicrob. Chemother.* **75**, 576–585.

Jiang, X., Liu, Y., Ma, L., Ji, R., Qu, Y., Xin, Y., and Lv, G. 2018. Chemopreventive activity of sulforaphane. *Drug Des. Devel. Ther.* **12**, 2905–2913.

Johansson, N.L., Pavia, C.S., and Chiao, J.W. 2008. Growth inhibition of a spectrum of bacterial and fungal pathogens by sulforaphane, an isothiocyanate product found in broccoli and other cruciferous vegetables. *Planta Med.* **74**, 747–750.

Kaufmann, S.H.E., Dorhoi, A., Hotchkiss, R.S., and Bartenschlager, R. 2018. Host-directed therapies for bacterial and viral infections. *Nat. Rev. Drug Discov.* **17**, 35–56.

Keren, I., Wu, Y., Inocencio, J., Mulcahy, L.R., and Lewis, K. 2013. Killing by bactericidal antibiotics does not depend on reactive oxygen species. *Science* **339**, 1213–1216.

Kilinç, G., Saris, A., Ottenhoff, T.H.M., and Haks, M.C. 2021. Host-directed therapy to combat mycobacterial infections. *Immunol. Rev.* **301**, 62–83.

Kohanski, M.A., Dwyer, D.J., Hayete, B., Lawrence, C.A., and Collins, J.J. 2007. A common mechanism of cellular death induced by bactericidal antibiotics. *Cell* **130**, 797–810.

Kumar, A., Farhana, A., Guidry, L., Saini, V., Hondalus, M., and Steyn, A.J.C. 2011. Redox homeostasis in mycobacteria: the key to tuberculosis control? *Expert Rev. Mol. Med.* **13**, e39.

Kumar, A., Toledo, J.C., Patel, R.P., Lancaster, J.R.Jr, and Steyn, A.J. 2007. *Mycobacterium tuberculosis* DosS is a redox sensor and DosT is a hypoxia sensor. *Proc. Natl. Acad. Sci. USA* **104**, 11568–11573.

Lee, W. and Lee, D.G. 2014. Lycopene-induced hydroxyl radical causes oxidative DNA damage in *Escherichia coli*. *J. Microbiol. Biotechnol.* **24**, 1232–1237.

Li, D., Shao, R., Wang, N., Zhou, N., Du, K., Shi, J., Wang, Y., Zhao, Z., Ye, X., Zhang, X., *et al.* 2021. Sulforaphane activates a lysosome-dependent transcriptional program to mitigate oxidative stress. *Autophagy* **17**, 872–887.

Liu, Y. and Imlay, J.A. 2013. Cell death from antibiotics without the involvement of reactive oxygen species. *Science* **339**, 1210–1213.

Mo, S., Liu, X., Zhang, K., Wang, W., Cai, Y., Ouyang, Q., Zhu, C., Lin, D., Wan, H., Li, D., *et al.* 2021. Flunarizine suppresses *Mycobacterium tuberculosis* growth via calmodulin-dependent phagosome maturation. *J. Leukoc. Biol.* **111**, 1021–1029.

Ouyang, Q., Zhang, K., Lin, D., Feng, C.G., Cai, Y., and Chen, X. 2020. Bazedoxifene suppresses intracellular *Mycobacterium tuberculosis* growth by enhancing autophagy. *mSphere* **5**, e00124-20.

Palucci, I. and Delogu, G. 2018. Host directed therapies for tuberculosis: futures strategies for an ancient disease. *Chemotherapy* **63**, 172–180.

Pei, Z., Wu, K., Li, Z., Li, C., Zeng, L., Li, F., Pei, N., Liu, H., Zhang, S.L., Song, Y.Z., *et al.* 2019. Pharmacologic ascorbate as a prodrug for hydrogen peroxide release to kill mycobacteria. *Biomed. Pharmacother.* **109**, 2119–2127.

Piasecka, A., Jedrzejczak-Rey, N., and Bednarek, P. 2015. Secondary metabolites in plant innate immunity: conserved function of divergent chemicals. *New Phytol.* **206**, 948–964.

Singh, V. and Chibale, K. 2021. Strategies to combat multi-drug resistance in tuberculosis. *Acc. Chem. Res.* **54**, 2361–2376.

Taati Moghadam, M., Amirmozafari, N., Shariati, A., Hallajzadeh, M., Mirkalantari, S., Khoshbayan, A., and Masjedian Jazi, F. 2020. How phages overcome the challenges of drug resistant bacteria in clinical infections. *Infect. Drug Resist.* **13**, 45–61.

Tian, X., Jiang, X., Welch, C., Croley, T.R., Wong, T.Y., Chen, C., Fan, S., Chong, Y., Li, R., Ge, C., *et al.* 2018. Bactericidal effects of silver nanoparticles on lactobacilli and the underlying mechanism. *ACS Appl. Mater. Interfaces* **10**, 8443–8450.

Vanduchova, A., Anzenbacher, P., and Anzenbacherova, E. 2019. Isothiocyanate from broccoli, sulforaphane, and its properties. *J. Med. Food* **22**, 121–126.

Vilchèze, C., Hartman, T., Weinrick, B., and Jacobs, W.R.Jr. 2013. *Mycobacterium tuberculosis* is extraordinarily sensitive to killing by a vitamin C-induced Fenton reaction. *Nat. Commun.* **4**, 1881.

Wang, G., Hong, Y., Johnson, M.K., and Maier, R.J. 2006. Lipid peroxidation as a source of oxidative damage in *Helicobacter pylori*: protective roles of peroxiredoxins. *Biochim. Biophys. Acta* **1760**, 1596–1603.

Wang, Y., Mandal, A.K., Son, Y.O., Pratheeshkumar, P., Wise, J.T.F., Wang, L., Zhang, Z., Shi, X., and Chen, Z. 2018. Roles of ROS, Nrf2, and autophagy in cadmium-carcinogenesis and its prevention by sulforaphane. *Toxicol. Appl. Pharmacol.* **353**, 23–30.

Wang, W., Yang, J., Zhang, J., Liu, Y.X., Tian, C., Qu, B., Gao, C., Xin, P., Cheng, S., Zhang, W., *et al.* 2020. An *Arabidopsis* secondary metabolite directly targets expression of the bacterial type III secretion system to inhibit bacterial virulence. *Cell Host Microbe* **27**, 601–613.

Warner, D.F. and Mizrahi, V. 2006. Tuberculosis chemotherapy: the influence of bacillary stress and damage response pathways on drug efficacy. *Clin. Microbiol. Rev.* **19**, 558–570.

Wayne, L.G. and Hayes, L.G. 1996. An *in vitro* model for sequential study of shiftdown of *Mycobacterium tuberculosis* through two stages of nonreplicating persistence. *Infect. Immun.* **64**, 2062–2069.

World Health Organization, WHO. 2021. Global tuberculosis report 2020. World Health Organization, Geneva, Switzerland.

Xie, Z., Siddiqi, N., and Rubin, E.J. 2005. Differential antibiotic susceptibilities of starved *Mycobacterium tuberculosis* isolates. *Antimicrob. Agents Chemother.* **49**, 4778–4780.

Zumla, A., Nahid, P., and Cole, S.T. 2013. Advances in the development of new tuberculosis drugs and treatment regimens. *Nat. Rev. Drug Discov.* **12**, 388–404.